


Title: Creep Failure Analysis for Ceramic Composites
Containing Viscous Interfaces

CONF-980627--

Author(s): Irene J. Beyerlein, CMS
Linan An, Univ. of Colorado
Rishi Raj, Univ. of Colorado

DISTRIBUTION OF THIS DOCUMENT IS UNLIMITED 

Submitted to: Society of Experimental Mechanics Conference
Houston, TX
June 1-3, 1998

MASTER

Los Alamos
NATIONAL LABORATORY

Los Alamos National Laboratory, an affirmative action/equal opportunity employer, is operated by the University of California for the U.S. Department of Energy under contract W-7405-ENG-36. By acceptance of this article, the publisher recognizes that the U.S. Government retains a nonexclusive, royalty-free license to publish or reproduce the published form of this contribution, or to allow others to do so, for U.S. Government purposes. The Los Alamos National Laboratory requests that the publisher identify this article as work performed under the auspices of the U.S. Department of Energy.

DISCLAIMER

This report was prepared as an account of work sponsored by an agency of the United States Government. Neither the United States Government nor any agency thereof, nor any of their employees, makes any warranty, express or implied, or assumes any legal liability or responsibility for the accuracy, completeness, or usefulness of any information, apparatus, product, or process disclosed, or represents that its use would not infringe privately owned rights. Reference herein to any specific commercial product, process, or service by trade name, trademark, manufacturer, or otherwise does not necessarily constitute or imply its endorsement, recommendation, or favoring by the United States Government or any agency thereof. The views and opinions of authors expressed herein do not necessarily state or reflect those of the United States Government or any agency thereof.

DISCLAIMER

Portions of this document may be illegible in electronic image products. Images are produced from the best available original document.

Creep Failure Analysis For Ceramic Composites Containing Viscous Interfaces

Irene J. BEYERLEIN, Linan AN[†], Rishi RAJ[†]

Center for Materials Science, Los Alamos National Laboratory, Los Alamos, NM 87545

[†]Department of Mechanical Engineering, University of Colorado, Boulder, CO 80309

ABSTRACT. This paper describes an experimental and theoretical study of the creep fracture of advanced ceramic composites under steady axial tension. Such composites consist of a high fraction of elongated ceramic grains, varying substantially in aspect ratio and embedded in a glassy matrix phase. For creep testing, a model test system was prepared, which consisted of well-aligned elongated mica platelets (~60 vol%) and residual glass phase (~40 vol%) in its final heat-treatment stage. The creep curves of several specimens under various applied loads and at a temperature (800 °C) higher than the T_g of the glass matrix (~650 °C) were obtained up to creep fracture. Micrographs of the creep fracture surfaces revealed substantial grain pull-out and cavitation in the matrix phase with virtually no transgranular fracture. The objective of this work is to simulate the creep response and fracture based on the accumulation of localized void growth and microstructural parameters, using a computational mechanics technique, called viscous break interaction (VBI), developed to compute stress fields around strongly interacting fractures or voids in composites with fibrous microstructures. To simulate the creep process up to fracture, a Monte Carlo model is developed which couples VBI with a statistical description of grain length. Both the experimental and simulation results show that random lengths and random overlap of the aligned grains naturally lead to (i) local and microstructure-sensitive damage evolution up to ultimate failure and (ii) substantial variation in failure times of seemingly identical specimens.

INTRODUCTION. Advanced ceramics, such as polycrystalline Si_3N_4 , are being considered as promising candidates for numerous high-temperature structural applications due to their superior stiffness, strength, and creep resistance. To use them reliably, these composite structures are loaded in service at a substantial fraction of their fast-fracture strengths, such that in many cases, they do not fail instantaneously, undergo long-term creep, and eventually fail in creep-rupture (most often suddenly). Of all the possible failure mechanisms which can operate over creep lifetime, the primary mechanism in materials of interest in this study is the growth and local coalescence of pre-existing and successively, nucleated voids. Moreover, the characteristics of the strain versus time creep curves, such as minimum creep rate and time-to-fracture, obtained from apparently identical specimens under the same temperature and load, were extremely varied [1,2].

A major contributor to material breakdown is creep of the residual glass matrix in shear around voids, leading to grain boundary sliding and stress concentration enhancement. Creep fracture due to cavitation has been suppressed in superalloys by producing either high-aspect ratio grains, wherein grain boundaries are aligned parallel to loading or an entire component is made from a single crystal [3]. For

instance, recently developed *in-situ* reinforced composites, in which the Si_3N_4 grains grow into platelet or needle-like, elongated shapes due to the α - β phase transformation, exhibited excellent room temperature mechanical properties, such as high strength, Weibull modulus, and crack-growth resistance ($> 10 \text{ MPa}\cdot\text{m}^{1/2}$) [4]. Other efforts for improving high temperature creep resistance involve developing post-sintering heat-treatments for the crystallization of the glass phase. However, there is always a small amount of residual glass left, since complete crystallization of the glass is thermodynamically impossible [5].

Modeling the nonlinear relationship between microstructure and macroscopic creep response and lifetime heavily relies on the calculation of stress and displacement around randomly occurring and interacting failure events. When and where microscale failure progresses are governed by the time-varying stress redistribution around the current state of damage. Therefore simulating creep damage evolution in increasing time steps requires a *physically realistic and fast* stress calculation. In this work, we employ a recently developed computational mechanics technique, called viscous break interaction (VBI) [6], to quickly calculate the stress and displacements in response to closely interacting voids and concomitant creep of the viscous glass phase. Moreover, creep damage accumulation in its critical form tends to be *localized rather than uniformly distributed*. Therefore one of the difficulties in modeling progression of microscale failure events in larger composites is the broad range and statistical variation in the length- and time scales involved. This work initiates development of a Monte Carlo model which implements VBI to overcome such difficulties.

EXPERIMENTAL TESTING AND RESULTS. In the present paper, a commercially available, glass ceramic system was utilized since (i) a large number of samples were needed to capture statistical variation and (ii) its microstructure was similar to that of Si_3N_4 . These model composites were prepared by crystallizing the green glass obtained from Corning, Inc. It was found that an elongated grain structure can be obtained using a 2-step heating cycle: (1) green glass was heat-treated to 900 °C for 10 min to nucleate the mica phase and (2) samples were then heated to 950 °C for 2 hr for grain growth. To align the mica grains, 25 MPa was applied during the first step. The resultant total forged strain was ~1000%, and the final thickness of the forged disc was ~0.3 mm. In its final crystallized state, samples consisted of ~60 vol% mica platelets and ~40 vol% residual glass [1].

In a custom-designed small tube furnace, the creep tests on dogbone-shaped samples (4.3 mm gauge length) were conducted under tension dead-weight loading and at a temperature of 800 °C, a temperature higher than the glass transition temperature (T_g) of the residual glass (~650 °C).

The applied load was varied from 11 to 18 MPa. An LVDT (PR 750-050, Macro Sensors, Pennsauken, NJ) was attached to the load train for measuring displacement as a function of elapsed time, which was later used to determine the creep strain versus time curves and time-to-fracture for each specimen. The temperature profile of the furnace was measured with an independent thermocouple and was found to vary within 1°C from the set-point in the zone occupied by the sample. Several samples were tested to rupture under the same temperature and loading conditions. Only the data from samples which failed at a location away from the corners at the ends of the dogbone geometry were included in the data pool. In the end, at least 25 data points were collected for each applied load.

The test results revealed substantial variability in the creep response among 25 specimens at given test conditions. For example, the creep fracture curves for several specimens under 12.5 MPa are shown in Fig. 1, and clearly have pronounced variation, particularly in their minimum strain rate and time-to-fracture. At the higher loads tested, 12.5–18 MPa, the curves typically exhibited distinct primary, secondary, and tertiary stages of creep. However at relatively lower loads, e.g. 11 MPa, often there was no measurable tertiary stage. The latter response also occurs in Si_3N_4 [2]. The mean failure times (\pm standard deviation) at loads 11, 12.5, 15, and 18 MPa were 620 ± 356 , 122 ± 102 , 44 ± 73 , and 5.5 ± 3.3 min., respectively. Accordingly, the coefficient of variation (or ratio of standard deviation to mean) increased from 0.6, 0.85, to 1.7 with an increase in applied load from 11, 12.5, to 15 MPa and dropped to approximately 0.6 again at 18 MPa. This suggests a change in failure mode between the moderately loaded and highly loaded specimens. In the latter case, creep fracture occurred within 10 min. and exhibited weakest-link, brittle-like fracture; unlike those at lower loads, which had much longer lifetimes and underwent lower increases in strain after that achieved at the end of the primary stage. SEM micrographs of the creep fracture surfaces from all loads tested indicated that the primary fracture mechanism was the formation and coalescence of cavities within the glass phase, as opposed to grain fracture or extension from a pre-existing indentation flaw [1]. Therefore, we propose that likely origins of this variation are variations in grain lengths, grain overlap, and the initial spatial density of the cavities.

SIMULATION MODEL AND RESULTS. We first discuss the code for stress and displacement calculations, then describe the initial phase in our efforts to simulate creep fracture, and follow with some Monte Carlo simulation results. The present creep fracture simulations use a recently developed micromechanical computational technique, called viscous break interaction (VBI) [6] for the time-dependent stress and displacement calculations. VBI is built on the 2D shear-lag analysis for a multi-fiber composite [7], assuming that (i) the matrix is linearly viscous or linearly viscoelastic and creeps only in shear and (ii) the fibers, with time-independent, elastic properties, sustain all tensile load. VBI calculates spatial and temporal variations in stress and displacement along any grain or matrix region, which realistically will be different from the far-field and from those in neighboring regions. Despite continually increasing speed and memory capability of computer hardware, efficient computational mechanics techniques are still necessary and crucial for broad length scale stress and displacement calculations. For VBI, great efficiencies arise primarily because

computational effort is tied to the amount of damage (e.g. number of cavities), not composite volume, as in typical finite element schemes and random or spring network models.

To date, VBI has been formulated to efficiently handle a fairly large number of arbitrarily located fractures or cavities (or 'breaks') which are pre-existing and progress in time. Thus far, we have shown many interesting results from using VBI, such as (1) the distinctions in stress redistribution between large numbers of aligned breaks (transverse cracks or a finite and infinite row of short cracks) and a large process zone of staggered (misaligned) breaks, and (2) how the spatial arrangement and time growing interactions of several close breaks influence the local matrix creep rate and tensile stress redistribution in the grains, and macroscopically, the time scales of multiple creep stages in composite strain. We are now well-positioned to combine the experimental work with the micromechanical modeling and simulation work to understand how microstructural properties influence statistical creep fracture in advanced ceramics.

In application of the VBI technique to advanced ceramics, consisting of elongated grains in a glassy secondary phase near or above its T_g , we assume the matrix creeps as a linearly viscous (Newtonian) material. Therefore, the matrix creep compliance $J(\mathcal{T})$, apart from the initial elastic response, is a linear function of time,

$$J(\mathcal{T}) = J_e(\mathcal{T}/\mathcal{T}_c) \quad (1)$$

where \mathcal{T} is real time and \mathcal{T}_c is the characteristic time constant for matrix relaxation. Since we have neglected the initial elastic component of the matrix compliance, the constant J_e , which has dimensions [stress^{-1}], becomes reminiscent of this time-independent compliance. That is, when time $\mathcal{T} = \mathcal{T}_c$, the creep strain is J_e . According to (1), the matrix has a constant viscosity $\eta = \mathcal{T}_c J_e$. In the VBI formulation, length, time, stresses and displacements are normalized by the dimensions and moduli of the grains and glassy phase and η . Relevant to the present work, the normalizations for real time \mathcal{T} , and axial length x (along the grain direction) are

$$\xi = \frac{x}{w\sqrt{EJ_e}}, \quad (2)$$

and

$$t = \frac{\mathcal{T}}{\mathcal{T}_c} = \frac{\mathcal{T}}{\eta J_e}, \quad (3)$$

where E is the Young's modulus of the grains, and w is the surface-to-surface spacing between grains (see Fig. 3). Next, we introduce the model composite, referring the reader to [6] for a complete development of the VBI technique.

In this initial phase of modeling, the objective is to isolate the influence of statistical variation in grain size and coalescence of pre-existing voids. Fig. 2 shows a histogram of the axial grain lengths measured using several specimens. These results suggest that the lengths of the grains can range from less than 1 to 30 μm within any

specimen and has a mean around 14-15 μm . The microstructure is modeled as illustrated in Fig. 3, which shows a region within the infinitely long composite containing evenly spaced grains of random length aligned along the loading direction. In this early stage, this model is 2D and represents the microstructure seen from a side view of the dogbone specimen (i.e. grains in Fig. 3 are side view of platelets). Also on Fig. 3, the applied far field tensile load sustained by the ceramic grains, denoted p^* , is constant.

In the dogbone test specimen, there were approximately 80 to 100 grains through its thickness ($\sim 200 \mu\text{m}$), and therefore, we considered our model to contain 100 grains in the transverse direction. In the longitudinal direction, the microstructure of random length and overlapped grains, as shown in Fig. 3, is created by randomly placing the locations of grain ends along each of the 100 'axial grain regions', such that the distance between the ends (i.e. length of grains) varies between 0 and 28 μm . The resolution of these grain end positions are within a normalized length scale of 0.01. Apart from w , which is $\sim 1.0 \mu\text{m}$, the remaining material properties are unknown for this glass-ceramic system. Reasonable estimates were utilized in this study: $\eta = 10^{12}$ Poise (Nsec/m²), $E = 50$ GPa, and $J_e = 25$ GPa. Using these estimates and (2), the normalized grain lengths in the model composite range approximately from 0 to 20. In the longitudinal (or loading) direction, we considered this generated microstructure to exist only over a 70 μm length. This length was selected because in creep testing, void coalescence and propagation across the width of the specimen occurred within a localized band, which was typically 50-60 μm in length (or 1.2-1.4% of the gauge length). However, to properly compare simulation results to experiment, the full gauge length (4.3 mm) should be considered since the extremal, statistical nature of creep-rupture leads to a dependence of lifetime on specimen volume, or size-effect. In future work, VBI, reformulated for a finite length model, will be utilized in the fracture simulations.

As a result of numerous factors, some grain ends (or boundaries) will have properties susceptible for cavity nucleation and growth, depending on orientation with respect to loading direction and variations on composition, surface energy, diffusivity, and thickness of the boundary phase. Therefore susceptibility to cavitation not only depends on the local stresses, but also on a threshold stress, σ_0 . Also observations of small numbers of boundaries cavitated prior to loading suggests that these σ_0 strengths may be heterogeneous (that is, random). For simplicity and to isolate effects of random grain lengths, we set σ_0 , the stress required to nucleate and propagate a cavity across the entire grain width, to zero, and thus there will be no direct dependency on applied load. In an expanded paper, σ_0 will not only be nonzero, but random in the model, and as one consequence, a random, initial distribution of cavities will be generated when the tensile load is first applied, and new ones will evolve as cavity growth and time progress.

Several simulations were performed, wherein each realization includes a different spatial random distribution of grains (and cavities), giving rise to a distinct stress intensity evolution, creep strain curve, and fracture time. Under uniform tension, viscous deformation of the surrounding

matrix accommodates cavity opening separation, thereby causing overlapping grains to slip relative to their neighbors and nearby cavities to coalesce. As sliding and separation continue in time, the overall creep strain and strain rate increase, and eventually, along some statistically preferential plane, voids coalesce transversely across the entire composite, resulting in failure. In the simulation model, the time when this occurs is defined as the fracture time, t_f , and a time step was selected small enough to not affect the fracture time within 3 significant digits. Using the estimates for E , J_e , and η stated above, the relation between the real failure time and normalized one is $\mathcal{T}_f = (40 t_f)$ sec.

Lifetime distributions for 100 realizations for each case, one where the length of the granular microstructure is 70 μm and the other where this length is much shorter, 28 μm , are shown on a Weibull plot in Fig. 4. This Weibull plot plots the probability of creep fracture P versus t_f or $\mathcal{T}_f/\mathcal{T}_C$, using special coordinates, wherein the vertical axis is linear in $\ln(-\ln(1-P))$ and the horizontal axis in $\ln(\mathcal{T}_f/\mathcal{T}_C)$, so that a Weibull distribution will appear as a straight line. As shown, increasing the length of the granular microstructure from 28 to 70 μm decreases the mean failure time slightly and decreases the variation in the fracture time. Also, the simulated fracture times (ranging from 11.8 to 26.5 min) are significantly less than the actual test times, which is to be expected since the simulation is 2D and assumes all the grain ends are cavitated at time zero. Apart from needed extensions in the simulation code as mentioned above, other objectives for future work are to determine the form and parameters of these lifetime distributions, which is clearly not Weibull (and also not lognormal or Guassian). These goals are within reach through systematically building representative simulation models to reveal the non-intuitive, complex processes of creep fracture and guide in the analytical probability modeling.

REFERENCES

- [1] An, L. a & Raj, R. "Variability of time-to-fracture in fibrous glass-ceramics at high temperatures", Submitted (1998).
- [2] Menon, M. N., More, K. L., Hubbard, C. R., and Nolan, T. A. "Creep and stress rupture behavior of an advanced silicon nitride: Part I, Experimental Observations" *J. Amer. Ceram. Soc.*, **77**, 1217-1227 (1994).
- [3] Ross, E.W. & Sims, C.T. "Nickle-Based Alloys," in *Superalloys II*, 97-131, Wiley, New York (1987).
- [4] Li, C.W. & Yamanis, J. "Super-Tough Silicon Nitride with R-Curve Behavior," *Ceram. Eng. Sci. P.*, **10**, 632-45 (1989).
- [5] Raj, R. & Lange, F. F. "Crystallization of Small Quantities of Glass (or a Liquid) Seggregated in Grain Boundaries," *Acta Metall. Mater.*, **40** [9] 2233-45 (1992).
- [6] Beyerlein, I. J., S. L. Phoenix & R. Raj. "Time evolution of stress redistribution around multiple fiber breaks in a composite with viscous and viscoelastic matrices." To appear in *Int. J. Solids Structures*, (1997).
- [7] Hedgepeth, J. M. "Stress concentrations in filamentary structures". *NASA TN D-882* (1961).

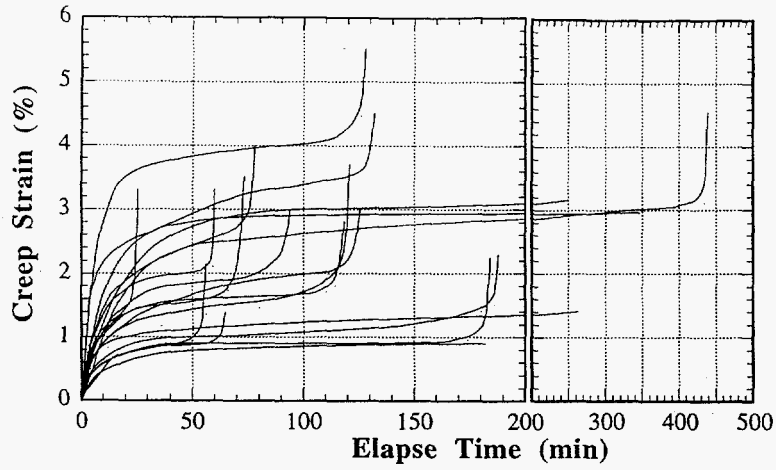


Fig. 1 Creep fracture curves of several similar specimens under 800 °C and 12.5 MPa.

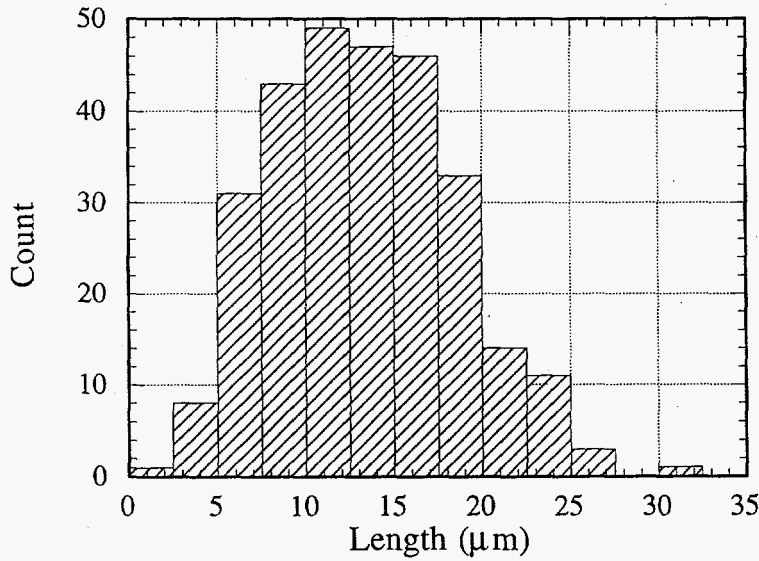


Fig. 2 Histogram of grain lengths within microstructure of our model glass-ceramic system.

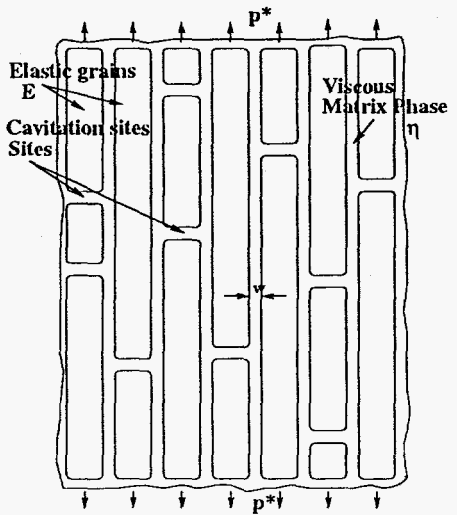


Fig. 3 Model composite geometry with randomly overlapping and random length grains.

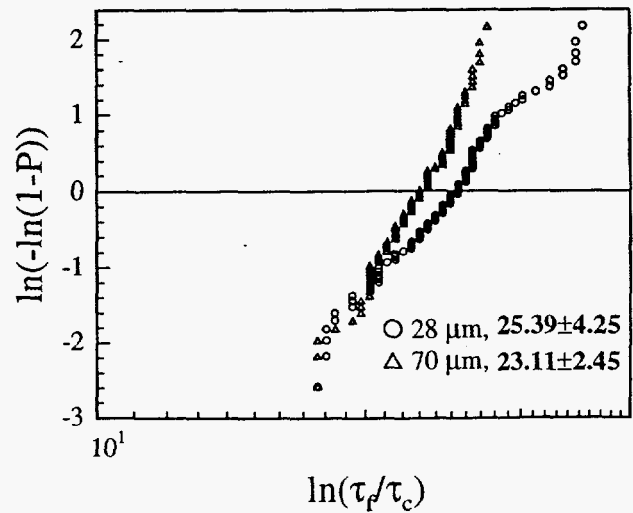


Fig. 4 Weibull plot of simulated fracture times for 2D model composite of two lengths.